CHINESE OPTICS LETTERS

Vol. 21, No. 2 | February 2023

Single-lane 200 Gbit/s photonic wireless transmission of multicarrier 64-QAM signals at 300 GHz over 30 m

Hongqi Zhang (张红旗)[1,2], Lu Zhang (张 鹿)[1,2], Zuomin Yang (杨作民)[2], Hang Yang (杨 航)[2], Zhidong Lü (吕治东)[2], Xiaodan Pang (庞晓丹)[3], Oskars Ozolins[3,4], and Xianbin Yu (余显斌)[1,2*]

[1] Zhejiang Lab, Hangzhou 311121, China

[2] College of Information Science and Electronic Engineering, Zhejiang University, Hangzhou 310027, China

[3] Applied Physics Department, KTH Royal Institute of Technology, 10691 Stockholm, Sweden

[4] Networks Unit, RISE Research Institutes of Sweden, 16440 Kista, Sweden

*Corresponding author: xyu@zju.edu.cn

Received July 27, 2022 | Accepted September 8, 2022 | Posted Online November 11, 2022

Recently, wireless communication capacity has been witnessing unprecedented growth. Benefits from the optoelectronic components with large bandwidth, photonics-assisted terahertz (THz) communication links have been extensively developed to accommodate the upcoming wireless transmission with a high data rate. However, limited by the available signal-to-noise ratio and THz component bandwidth, single-lane transmission of beyond 100 Gbit/s data rate using a single pair of THz transceivers is still very challenging. In this study, a multicarrier THz photonic wireless communication link in the 300 GHz band is proposed and experimentally demonstrated. Enabled by subcarrier multiplexing, spectrally efficient modulation format, well-tailored digital signal processing routine, and broadband THz transceivers, a line rate of 72 Gbit/s over a wireless distance of 30 m is successfully demonstrated, resulting in a total net transmission capacity of up to 202.5 Gbit/s. The single-lane transmission of beyond 200 Gbit/s overall data rate with a single pair of transceivers at 300 GHz is considered a significant step toward a viable photonics-assisted solution for the next-generation information and communication technology (ICT) infrastructure.

Keywords: terahertz communication; terahertz photonics; wavelength division multiplexing; photonic-wireless transmission.
DOI: 10.3788/COL202321.023901

1. Introduction

In recent years, the explosive growth of the demand for wireless capacity has been well-witnessed in both wired and wireless communications, driven by the increased number of Internet end users. It is foreseen that the trend seems likely to continue over the next decade[1]. To meet the requirements of the increasing data capacity, wireless transmission beyond 100 Gbit/s and even Tbit/s is essential[2]. It is hard to obtain such high data rates for current wireless communication in the millimeter-wave or microwave regions due to the limited available bandwidth. In this sense, researchers' attention has naturally shifted to the terahertz (THz) region (0.3–10 THz), which features large available bandwidth to satisfy the increasing demand for wireless communication traffic[3]. Currently, extensive efforts have been made in the evolution of THz communication to deliver high transmission capacity[4–6].

Among the previously reported THz wireless communication systems, photonics-aided THz communication links clearly show some advantages. First, it is compatible to drive THz transmitters remotely through low-loss optical fibers and hence can be seamlessly connected to the existing fiber-optic network. Moreover, it is straightforward for the photonics-aided communication link to employ flexible carrier switching, complex modulation formats, multicarrier modulation, and so on[7]. As a result, photonics-assisted THz communications are thereby under rapid development. Initially, for instance, the work on 300 GHz wireless demonstration of 50 Gbit/s over 100 m with on–off keying (OOK) modulation format[8] and 100 Gbit/s over 0.1 m with quadrature-phase-shift-keying (QPSK) modulation format[9] is presented. Then 16-ary quadrature amplitude modulation (16-QAM) format has also been adopted to increase spectral efficiency, resulting in photonic wireless experimental demonstrations of 100 Gbit/s in the 350 GHz band[10] and 128 Gbit/s in the 300 GHz band[11]. However, restrained by the emission power of the opto-electronic transmitter, the wireless distance and data rates are restrained. Subsequently, the probabilistic shaping (PS) technique has alternatively been employed in THz photonic wireless communication systems to improve the energy consumption per bit. For example,

132 Gbit/s PS 64-QAM at 400 GHz over 1.8 m and 100 Gbit/s at 350 GHz over 26.8 m have been achieved[12,13].

In addition, some more advanced modulation and multiplexing techniques have also been used in THz photonic wireless communication links, such as 131 Gbit/s orthogonal frequency division multiplexing (OFDM) at 408 GHz over 10.7 m[15], wavelength division multiplexing (WDM) 260 Gbit/s at 300–500 GHz over 0.5 m[16], and 600 Gbit/s at 320–380 GHz over 2.8 m, combining WDM and the polarization multiplexing (PDM) method[17]. However, demonstrated simultaneous transmission rates over a single pair of THz transceivers are still below 200 Gbit/s, limited by the available THz receiver bandwidth and signal-to-noise ratio (SNR). The main challenges include weak opto-electronic THz emission power, high atmospheric propagation loss, and limited THz component bandwidth[18]. On the other hand, the multicarrier scheme shows some advantageous performance compared with single-carrier links in terms of spurious-free dynamic range (SFDR) and noise figure (NF)[19], which can be expected to benefit a THz photonic link. Therefore, we propose combining these advanced techniques, including carrier multiplexing, high-order QAM modulation formats, and well-tailored digital signal processing, to push the single-lane data rate beyond the state-of-the-art envelope in the THz band. Recent development progress on photonic THz communication above 300 GHz is summarized in Table 1.

In this work, we employ a broadband unitraveling carrier photodiode (UTC-PD, 100 GHz bandwidth)[20] with fast response time, high output saturation current, and high opto-electronic conversion efficiency to generate the THz signals. A Schottky diode mixer downconverts the wireless THz signals to the intermediate frequency (IF) signals. Combining carrier multiplexing, ultrabroadband THz transceivers, well-tailored digital signal processing (DSP) routines, and high-order QAM modulation formats, we experimentally demonstrated a total net transmission capacity of up to 202.5 Gbit/s over 30 m.

Table 1. Development Progress on Photonic THz Communication.

Carrier (GHz)	Data Rate per Lane (Gbit/s)	Modulation Format	Transmission Distance (m)	Ref.
300	50	OOK	100	[8]
300	100	QPSK	0.1	[9]
350	100	16-QAM	2	[10]
300	128		0.5	[11]
450	132	PS-64-QAM	1.8	[12]
350	100.8	16-QAM-OFDM	26.8	[13]
408	131		10.7	[14]
300–500	80	16-QAM	0.5	[15]
320–380	155	PS-64-QAM-OFDM	2.8	[16]
300	202.5	64-QAM	30	This work

2. Experimental Setup

As a proof-of-concept experiment, the configuration of the multicarrier THz wireless link is depicted in Fig. 1(a). To begin with, we employ an external cavity laser (ECL1) to generate a laser beam located at 193.417 THz. Subsequently, the optical carrier is fed into an optical in-phase and quadrature-phase modulator (IQ-MOD, 60 GHz bandwidth) to carry out the baseband signal modulation (64-QAM), and the polarization of optical signal from the ECL1 with the IQ-MOD is aligned by a polarization controller (PC1). In this demonstration, a pseudo-random binary sequence (PRBS-15) is generated from an arbitrary waveform generator (AWG, Keysight M8194, 120 GSa/s). To reduce the intersymbol interference, a root-raised cosine (RRC) filter is employed to pulse-shape the baseband transmitting samples. An erbium-doped fiber amplifier (EDFA) is then used to amplify the modulated optical signals, and the spontaneous emission (ASE) noise from the EDFA is suppressed by a bandpass optical filter. Subsequently, the three free-running optical local oscillators (LOs), i.e., Lasers 2, 3, and 4, are centered at 193.7035, 193.7165, and 193.7295 THz, respectively. A 3 × 1 optical coupler combines these three lasers, each with 200 kHz linewidth. Then the filtered optical signal is coupled with combined output modulated optical signals by a 50:50 optical coupler. The output power of the three LO light beams is 15 dBm, which is

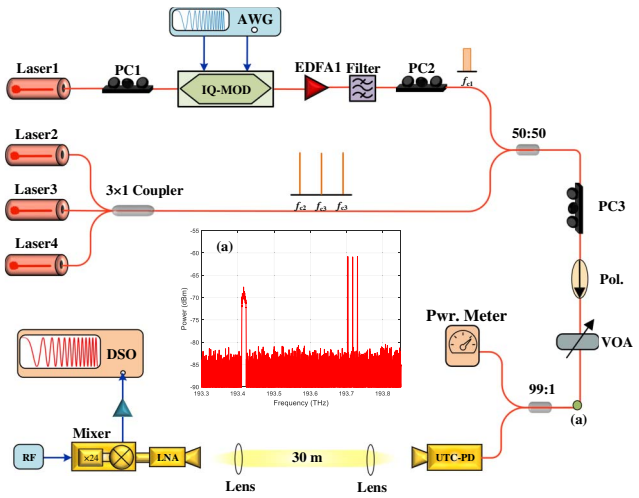

Fig. 1. Experimental configuration of the multicarrier photonics wireless transmission link. PC, polarization controller; IQ-MOD, in-phase and quadrature modulator; UTC-PD, unitraveling carrier photodiode; AWG, arbitrary waveform generator; LNA, low-noise amplifier; EDFA, erbium-doped fiber amplifier; VOA, variable optical attenuator; Pol., polarizer; DSO, digital storage oscilloscope; LO, local oscillator; inset (a), optical spectrum after the 50:50 optical coupler.

power-balanced with the filtered optical signal. To maximize the responsivity of a UTC-PD (100 GHz bandwidth), the polarizer (Pol.) and a PC3 are used to align the polarization. In addition, we used a variable optical attenuator (VOA) to control the incident optical power to the UTC-PD. Then the output signal is sent to a 99:1 optical coupler to monitor the optical power entering the UTC-PD to protect the device. After that, the optical signal is fed into the UTC-PD for heterodyne generation of a three-subcarrier THz-modulated signal. The inset illustrates the optical spectra after the 50:50 optical coupler.

After photomixing in the UTC-PD, three THz signals located at 286.5, 299.5, and 312.5 GHz, named subcarrier_1 (SC_1), subcarrier_2 (SC_2), and subcarrier_3 (SC_3), are generated separately. Figure 2(a) shows the electrical spectrum of the three modulated signals in the THz regions. The modulated data in all three SCs are identical and are not decorrelated due to experimental constraints. However, due to sufficient channel separation and limited coherent cross talk between the channels, we could expect only marginal discrepancies in the overall transmission performance after proper channel decorrelation.

The THz signals are then radiated into free space via a horn antenna and propagate through a 30 m line-of-sight (LOS) free-space link. The wireless distance is obtained with a reflective mirror placed 15 m away from the transmitter and the receiver. A picture of the experimental setup is depicted in Fig. 2(b). After that, the THz beam is collimated and focused by 25 dBi gain THz lenses. After the 30 m wireless transmission, the three-subcarrier modulated signals are first amplified by a low-noise amplifier (LNA, 250–350 GHz, 25 dB gain). Then a Schottky diodes mixer (VDI WR3.4, 220–330 GHz, 40 GHz bandwidth) simultaneously downconverted the three subcarriers to the IF domain. The amplitude and frequency of the LO signal are −2 dBm and 280 GHz, respectively. The LO signal mixed with the three THz signals, and the IF modulated signals located at 6.5, 19.5, and 32.5 GHz are then obtained. In this demonstration, the total occupied bandwidth of the modulated signal is 39 GHz, which is within the detectable IF bandwidth of the mixer (40 GHz), enabling simultaneous reception of three-subcarrier signals. Subsequently, the IF modulated signals are sampled by a 160 GSa/s real-time oscilloscope and are demodulated with offline DSP.

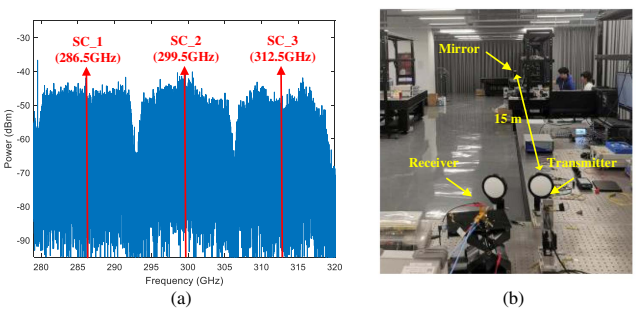

Fig. 2. (a) Electrical spectrum of 64-QAM signals before downconversion; (b) picture of experimental setup.

At the transmitter side, the electrical fields at the output of Lasers 1–4 are expressed as

$$E_i(t) = \sqrt{P_i} \cdot \exp\{-j[\omega_i t + \varphi_i(t)]\}, \qquad i = 1, 2, 3, 4, \tag{1}$$

where P_i, ω_i, φ_i are the power, angular frequency, and phase of the lasers, respectively. After the optical modulation of the IQ-MOD, the output electrical field of Laser 1 is given as

$$E_1(t) = \sqrt{P_1} \cdot [I(t) + jQ(t)] \cdot \exp\{-j[\omega_1 t + \varphi_1(t)]\}, \tag{2}$$

where $I(t)$, $Q(t)$ are the in-phase and quadrature components of the baseband signal, respectively. At the output of UTC-PD, the generated THz radiation is given as

$$\begin{aligned} E_{\mathrm{THz}}(t) &= \sum_{i=1}^{4} E_{i(t)} \cdot \mathrm{conj}\left[\sum_{i=1}^{4} E_{i(t)}\right], \qquad i = 1, 2, 3, 4, \\ &\propto \sum_{k=2}^{4} \sqrt{P_1 P_k} \cos[(\omega_k - \omega_1)t + \varphi_k(t) - \varphi_1(t)] \\ &\quad k = 2, 3, 4. \end{aligned} \tag{3}$$

From Eq. (3), three THz signals are generated. At the receiver side, the THz signals are downconverted into the IF domain. The electrical field of the LO signal is $E_{\mathrm{LO}}(t) = \sqrt{P_{\mathrm{LO}}} \cdot \exp\{-j[\omega_{\mathrm{LO}} t + \varphi_{\mathrm{LO}}(t)]\}$, and P_{LO}, ω_{LO}, φ_{LO} are the power, angular frequency, and phase of the LO signal, respectively. After mixing by the THz mixer, the output IF signal is given as

$$\begin{aligned} E_{\mathrm{IF}}(t) &= E_{\mathrm{THz}}(t) \cdot E_{\mathrm{LO}}(t) \\ &\propto \sum_{k=2}^{4} \sqrt{P_1 P_k P_{\mathrm{LO}}} \cos[(\omega_k - \omega_1 - \omega_{\mathrm{LO}})t \\ &\quad + \varphi_k(t) - \varphi_1(t) - \varphi_{\mathrm{LO}}(t)], \qquad k = 2, 3, 4. \end{aligned} \tag{4}$$

From Eq. (4), three subcarriers are generated at the output of the THz mixer. Then the signals are sampled by a real-time oscilloscope and demodulated with our well-defined DSP routine.

The link budget can be calculated according to the Friis formula[21], which is expressed as

$$P_{\mathrm{Rx}} = P_{\mathrm{Tx}} + G_{\mathrm{Tx}} + G_{\mathrm{Rx}} - L_{\mathrm{loss}}, \tag{5}$$

where P_{Rx} is the received THz power, P_{Tx} is the transmitted THz power from the UTC-PD, and G_{Tx} and G_{Rx} are the directional gains of the THz antennas at the transmitter and receiver, respectively. L_{loss} is the free-space path loss, which is expressed as

$$L_{\mathrm{loss}} = 20 \log \frac{4\pi df}{c}, \tag{6}$$

where d is the wireless transmission distance from the transmitter to the receiver, f is the operating frequency of the THz signal,

Table 2. Link Parameters of Our Communication System.

Link Parameters	Value
Operating frequency	300 GHz
Radiation THz power	−13 dBm
Tx antenna directional gain	25 dBi
Tx antenna convergence gain	20 dBi
Free-space path loss	111.5 dB
Rx antenna convergence gain	20 dBi
Rx antenna directional gain	25 dBi
LNA gain	25 dB
Conversion loss	12 dB
Baseband amplified gain	12 dB

and c is the speed of light in vacuum. In this demonstration, the wireless distance is 30 m, the operating frequency is 300 GHz, and the corresponding free-space path loss is 111.5 dB. Table 2 shows the link parameters of our communication system.

In the well-defined DSP routine, we employ three digital mixers located at 6.5, 19.5, and 32.5 GHz to separately downconvert the received three-subcarrier digital signal to the baseband. The digital mixers consist of a low-pass filter, a DC block, and a digital downconverter[22]. Subsequently, a Gram–Schmidt algorithm compensates for the IQ imbalance[23]. Then we employ a time-recovery algorithm based on maximum variance to resample the baseband signal to one sample per symbol (12 Gbaud). We employ the multimodulus algorithm (MMA) to converge the linear adaptive equalizer[24]. The Viterbi algorithm[25] and blind-phase search method[26] are used to compensate for the frequency offset and phase noise, respectively. In the experiment, the threshold of soft decision forward error correction (SD-FEC) with 20% overhead[27] and hard decision forward error correction (HD-FEC) with 6.25% overhead[28] is 2.7×10^{-2} and 4.5×10^{-3}, respectively.

3. Results and Discussions

Figure 3 depicts the bit error rate (BER) performance of the three subcarriers after 30 m wireless link. From Fig. 3, one can observe that the transmission performance of each subcarrier improves with the increasing input optical power, and all the transmission performance of the three subcarriers can reach the HD-FEC threshold with 6.25% overhead. In this case, three subcarriers carry an overall transmission capacity of 12 Gbaud × 3 subcarriers × 6 (bit/s)/Hz = 216 Gbit/s. Subtracting the FEC overhead, we achieved a net transmission capacity of 202.5 Gbit/s after 30 m wireless link. In addition, all transmissions through the

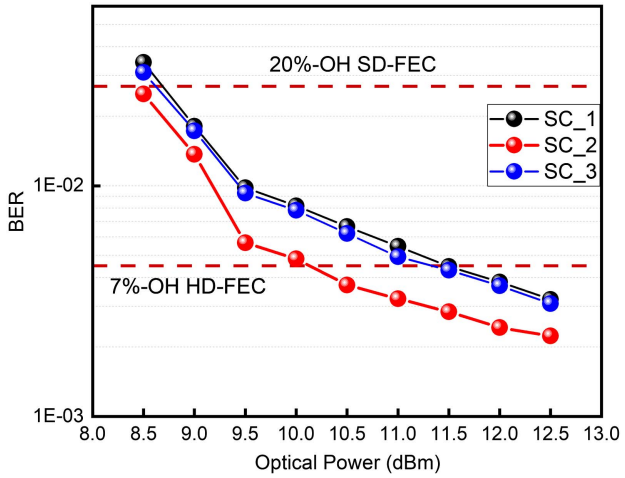

Fig. 3. Measured BER performance of three subcarriers after 30 m wireless transmission.

three THz subcarriers can reach the FEC threshold when the incident optical power is fixed at 11.5 dBm. Moreover, the transmission performance of SC_2 is better than that of SC_1 and SC_3 because the optimal responsivity of the UTC-PD is specified around the SC_2 frequency.

In the experiment, the performance of the photonics THz wireless link at different baud rates is further evaluated when the incident optical power is fixed at 12.5 dBm. The BER performance of the three subcarriers with baud rates from 2 to 12 Gbaud is depicted in Fig. 4(a). One can observe that the transmission performance decreases with the increasing baud rate.

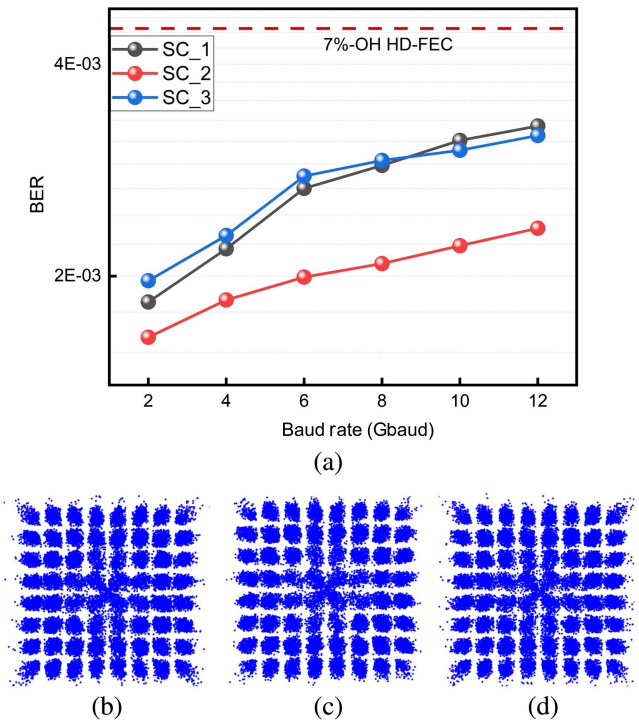

Fig. 4. (a) Measured BER performance with increasing baud rate of three subcarriers; (b)–(d) constellation of SC_1, SC_2, and SC_3 at 12 Gbaud.

Under the fixed emission power, the increasing baud rates result in the decrease of electrical SNR. The constellation diagrams of the three subcarriers at 12 Gbaud are depicted in Figs. 4(b)–4(d), and the BERs for the three subcarriers are 3.2×10^{-3}, 2.3×10^{-3}, and 3.1×10^{-3}, respectively.

4. Conclusion

In conclusion, a THz communication link simultaneously supporting three subcarriers of 64-QAM modulation format in the 300 GHz region is experimentally obtained. A single-lane aggregated data rate of 216 Gbit/s over 30 m is successfully achieved by employing a single THz emitter and receiver pair, corresponding to a net transmission capacity of 202.5 Gbit/s. The key enabling techniques include spectrally efficient modulation format, subcarrier multiplexing, well-tailored DSP algorithms, and broadband THz transceivers. This achievement pushes the high-speed photonics THz communication beyond the state of the art, which boosts the evolution of next-generation wireless communications.

Acknowledgement

This work was supported by the National Key Research and Development Program of China (Nos. 2020YFB1805700, 2018YFB1801503, and 2021YFB2800805), the National Natural Science Foundation of China (No. 62101483), the Natural Science Foundation of Zhejiang Province (No. LQ21F010015), and the Zhejiang Lab (No. 2020LC0AD01).

References

1. https://www.cisco.com/c/en/us/solutions/collateral/executive-perspectives/annual-internet-report/white-paper-c11-741490.html
2. G. Fettweis, F. Guderian, and S. Krone, "Entering the path towards terabit/s wireless links," in *Design, Automation & Test in Europe* (2011), p. 1.
3. V. Petrov, A. Pyattaev, D. Moltchanov, and Y. K. Koucheryavy, "Terahertz band communications: applications, research challenges, and standardization activities," in *2016 8th International Congress on Ultra Modern Telecommunications and Control Systems and Workshops* (2016), p. 183.
4. H.-J. Song and T. Nagatsuma, "Present and future of terahertz communications," IEEE Trans. Terahertz Sci. Technol. **1**, 256 (2011).
5. X. Yu, S. Jia, H. Hu, M. Galili, T. Morioka, P. U. Jepsen, and L. K. Oxenløwe, "160 Gbit/s photonics wireless transmission in the 300–500 GHz band," APL Photonics **1**, 081301 (2016).
6. L. Zhang, X. Pang, S. Jia, S. Wang, and X. Yu, "Beyond 100 Gb/s optoelectronic terahertz communications: key technologies and directions," IEEE Commun. Mag. **58**, 38 (2020).
7. T. Nagatsuma, G. Ducournau, Y. Yasuda, Y. Fujita, Y. Inubushi, S. Hisatake, A. M. Agoues, and G. C. Lopez, "Advances in terahertz communications accelerated by photonics," Nat. Photonics **10**, 371 (2016).
8. T. Nagatsuma, K. Oogimoto, Y. Yasuda, Y. Fujita, Y. Inubushi, S. Hisatake, A. M. Agoues, and G. C. Lopez, "300-GHz-band wireless transmission at 50 Gbit/s over 100 meters," in *41st International Conference on Infrared, Millimeter, and Terahertz waves (IRMMW-THz)* (2016), p. 1.
9. T. Nagatsuma, Y. Fujita, Y. Yasuda, Y. Kanai, S. Hisatake, M. Fujiwara, and J. Kani, "Real-time 100-Gbit/s QPSK transmission using photonics-based 300-GHz-band wireless link," in *IEEE International Topical Meeting on Microwave Photonics (MWP)* (2016), p. 27.
10. K. Liu, S. Jia, S. Wang, X. Pang, W. Li, S. Zheng, H. Chi, X. Jin, X. Zhang, and X. Yu, "100 Gbit/s THz photonic wireless transmission in the 350-GHz band with extended reach," IEEE Photon. Technol. Lett. **30**, 11 (2018).
11. C. Castro, S. Nellen, R. Elschner, I. Sackey, R. Emmerich, T. Merkle, B. Globisch, D. de Felipe, and C. Schubert, "32 GBd 16QAM wireless transmission in the 300 GHz Band using a PIN diode for THz upconversion," in *Optical Fiber Communication Conference (OFC)* (2019), paper M4F.5.
12. X. Li, J. Yu, L. Zhao, W. Zhou, K. Wang, M. Kong, G. Chang, Y. Zhang, X. Pan, and X. Xin, "132-Gb/s photonics-aided single-carrier wireless terahertz-wave signal transmission at 450 GHz enabled by 64QAM modulation and probabilistic shaping," in *Optical Fiber Communication Conference (OFC)* (2019), paper M4F.4.
13. S. Wang, Z. Lu, W. Li, S. Jia, L. Zhang, M. Qiao, X. Pang, N. Idrees, M. Saqlain, X. Cao, C. Lin, Q. Wu, X. Zhang, and X. Yu, "26.8-m THz wireless transmission of probabilistic shaping 16-QAM-OFDM signals," APL Photonics **5**, 056105 (2020).
14. S. Jia, M.-C. Lo, L. Zhang, O. Ozolins, A. Udalcovs, D. Kong, X. Pang, R. Guzman, X. Yu, S. Xiao, S. Popov, J. Chen, G. Carpintero, T. Morioka, H. Hu, and L. K. Oxenløwe, "Integrated dual-laser photonic chip for high-purity carrier generation enabling ultrafast terahertz wireless communications," Nat. Commun. **13**, 1388 (2022).
15. X. Pang, S. Jia, O. Ozolins, X. Yu, H. Hu, L. Marcon, P. Guan, F. Da Ros, S. Popov, G. Jacobsen, M. Galili, T. Morioka, D. Zibar, and L. K. Oxenløwe, "260 Gbit/s photonic-wireless link in the THz band," in *IEEE Photonics Conference* (2016), p. 1.
16. S. Jia, L. Zhang, S. Wang, W. Li, M. Qiao, Z. Lu, N. M. Idrees, X. Pang, H. Hu, X. Zhang, L. K. Oxenløwe, and X. Yu, "2 × 300 Gbit/s line rate PS-64QAM-OFDM THz photonic-wireless transmission," J. Light. Technol. **38**, 4715 (2020).
17. X. Yu, R. Asif, M. Piels, D. Zibar, M. Galili, T. Morioka, P. U. Jepsen, and L. K. Oxenløwe, "400-GHz wireless transmission of 60-Gb/s Nyquist-QPSK signals using UTC-PD and heterodyne mixer," IEEE Trans. THz Sci. Technol. **6**, 765 (2016).
18. L. Zhang, M. Qiao, S. Wang, Z. Lu, L. Zhang, X. Pang, X. Zhang, and X. Yu, "Nonlinearity aware optoelectronic terahertz discrete multitone signal transmission with a zero-bias diode," Opt. Lett. **45**, 18 (2020).
19. J. M. Singley, V. J. Urick, J. F. Diehl, K. J. Williams, and F. Bucholtz, "Increased performance of single-channel analog photonic links enabled by optical wavelength-division multiplexing," IEEE Trans. Microw. Theory Tech. **67**, 1274 (2019).
20. T. Ishibashi, Y. Muramoto, T. Yoshimatsu, and H. Ito, "Unitraveling carrier photodiodes for terahertz applications," IEEE J. Sel. Top. Quantum Electron. **20**, 79 (2014).
21. H. T. Friis, "A note on a simple transmission formula," Proc. IRE **34**, 254 (1946).
22. X. Pang, A. Caballero, A. Dogadaev, V. Arlunno, L. Deng, R. Borkowski, J. S. Pedersen, D. Zibar, X. Yu, and I. T. Monroy, "25 Gbit/s QPSK hybrid fiber-wireless transmission in the W-band (75–110 GHz) with remote antenna unit for in-building wireless networks," IEEE Photon. J. **4**, 691 (2012).
23. I. Fatadin, S. J. Savory, and D. Ives, "Compensation of quadrature imbalance in an optical QPSK coherent receiver," IEEE Photon. Technol. Lett. **20**, 1733 (2008).
24. P. J. Winzer, A. H. Gnauck, C. R. Doerr, M. Magarini, and L. L. Buhl, "Spectrally efficient long-haul optical networking using 112-Gb/s polarization-multiplexed 16-QAM," J. Light. Technol. **28**, 547 (2010).
25. I. Fatadin and S. J. Savory, "Compensation of frequency offset for 16-QAM optical coherent systems using QPSK partitioning," IEEE Photon. Technol. Lett. **23**, 1246 (2011).
26. A. J. Viterbi and A. M. Viterbi, "Nonlinear estimation of PSK-modulated carrier phase with application to burst digital transmission," IEEE Trans. Inf. Theory **29**, 543 (1983).
27. D. Chang, F. Yu, Z. Xiao, N. Stojanovic, F. N. Hauske, Y. Cai, C. Xie, L. Li, X. Xu, and Q. Xiong, "LDPC convolutional codes using layered decoding algorithm for high speed coherent optical transmission," in *OFC/NFOEC* (2012), p. 1.
28. L. M. Zhang and F. R. Kschischang, "Staircase codes with 6% to 33% overhead," J. Light. Technol. **32**, 10 (2014).